

Knockout of microRNA-21 reduces biliary hyperplasia and liver fibrosis in cholestatic bile duct ligated mice

Lindsey L Kennedy^{1,2}, Fanyin Meng^{1,2,3}, Julie K Venter², Tianhao Zhou², Walker A Karstens³, Laura A Hargrove³, Nan Wu², Konstantina Kyritsi², John Greene⁴, Pietro Invernizzi^{5,6}, Francesca Bernuzzi^{5,6}, Shannon S Glaser^{1,2,3}, Heather L Francis^{1,2,3} and Gianfranco Alpini^{1,2,3,4}

Cholestasis is a condition that leads to chronic hepatobiliary inflammation, fibrosis, and eventually cirrhosis. Many microRNAs (miRs) are known to have a role in fibrosis progression; however, the role of miR-21 during cholestasis remains unknown. Therefore, the aim of this study was to elucidate the role of miR-21 during cholestasis-induced biliary hyperplasia and hepatic fibrosis. Wild-type (WT) and miR-21^{-/-} mice underwent Sham or bile duct ligation (BDL) for 1 week, before evaluating liver histology, biliary proliferation, hepatic stellate cell (HSC) activation, fibrotic response, and small mothers against decapentaplegic 7 (Smad-7) expression. *In vitro*, immortalized murine biliary cell lines (IMCLs) and human hepatic stellate cell line (hHSC) were treated with either miR-21 inhibitor or control before analyzing proliferation, apoptosis, and fibrotic responses. *In vivo*, the levels of miR-21 were increased in total liver and cholangiocytes after BDL, and loss of miR-21 decreased the amount of BDL-induced biliary proliferation and intrahepatic biliary mass. In addition, loss of miR-21 decreased BDL-induced HSC activation, collagen deposition, and expression of the fibrotic markers transforming growth factor- β 1 and α -smooth muscle actin. *In vitro*, IMCL and hHSCs treated with miR-21 inhibitor displayed decreased proliferation and expression of fibrotic markers and enhanced apoptosis when compared with control treated cells. Furthermore, mice lacking miR-21 show increased Smad-7 expression, which may be driving the decrease in biliary hyperplasia and hepatic fibrosis. During cholestatic injury, miR-21 is increased and leads to increased biliary proliferation and hepatic fibrosis. Local modulation of miR-21 may be a therapeutic option for patients with cholestasis.

Laboratory Investigation (2016) 96, 1256–1267; doi:10.1038/labinvest.2016.112; published online 24 October 2016

Cholangiocytes are the target of cholangiopathies, such as primary biliary cholangitis (PBC) and primary sclerosing cholangitis (PSC), which are associated with dysregulation of cholangiocyte proliferation/loss.^{1,2} Cholestasis occurs by the obstruction of intra- or extrahepatic bile ducts,³ and is characterized by bile ductular reaction and extensive fibrosis.^{3,4} The bile duct ligation (BDL) and multidrug resistance gene-2 knockout (Mdr2^{-/-}) mouse models mimic some features of PSC including biliary damage and liver fibrosis.^{5,6} Normally, cholangiocytes are mitotically quiescent, but following damage (such as cholestasis) they begin to proliferate to repair the biliary tree to compensate for damage and loss of functionality.^{7–11} Alongside this enhanced proliferative

capacity, liver fibrogenesis occurs by the excessive accumulation of extracellular matrix proteins secreted by various cell types including activated hepatic stellate cells (HSCs).^{12–14} HSCs can be activated through a number of different factors secreted from cholangiocytes, including transforming growth factor- β 1 (TGF- β 1).^{15,16} Following TGF- β 1 receptor activation, phosphorylation of the secondary messengers small mothers against decapentaplegic-2 and -3 (Smad-2/3) occurs, which allows translocation to the nucleus where Smad-2/3 binds to the transcription factor Smad-4 and allows for increased cellular proliferation and fibrotic response. The effects of Smad-2/3 can be inhibited by the inhibitory Smad-7.

¹Research, Central Texas Veterans Health Care System, Temple, TX, USA; ²Department of Medicine and Medical Physiology, Texas A&M Health Science Center, College of Medicine, Temple, TX, USA; ³Scott & White Digestive Disease Research Center, Baylor Scott & White Health, Temple, TX, USA; ⁴Operational Funds, Baylor Scott & White Health, Texas A&M Health Science Center, College of Medicine, Temple, TX, USA and ⁵Humanitas Clinical and Research Center, Rozzano, Italy

Correspondence: Dr G Alpini, PhD, Central Texas Veterans Health Care System, Texas A&M Health Science Center, Olin E Teague Medical Center, 1901 South 1st Street, Building 205, 1R60, Temple, TX 76504, USA.

E-mail: galpini@tamu.edu

⁶Current address: Program for Autoimmune Liver Diseases, International Center for Digestive Health, Department of Medicine and Surgery, University of Milan-Bicocca, Milan, Italy.

Received 13 July 2016; revised 22 September 2016; accepted 26 September 2016

MicroRNAs (miRs) are conserved, small (20–25 nucleotide) noncoding RNAs that regulate RNA silencing and post-translational regulation of gene expression.^{17–19} Following cholestatic injury there is a wide range of miRNAs that are downregulated; however, only a few miRNAs such as miR-199, miR-200, and miR-34 are upregulated.^{20–22} miR-21 is an ubiquitously expressed miRNA that is upregulated in many different cancer types.^{23,24} A previous study found that miR-21 increases fibrogenesis during an experimental model of non-alcoholic steatohepatitis via inhibition of Smad-7.²⁵

Previously, we have shown that miR-21 is upregulated in a model of alcoholic liver injury and decreases HSC apoptosis.²⁶ However, this study did not delve into the role of miR-21 on cholangiocytes during injury or HSC-promoted fibrosis. The role of miR-21 during cholestatic injury is largely unknown; therefore, we aimed to uncover the role of miR-21 during cholestatic injury.

MATERIALS AND METHODS

Materials

All reagents were obtained from Sigma-Aldrich (St Louis, MO, USA), unless otherwise indicated. Cell culture reagents and media were obtained from Invitrogen Corporation (Carlsbad, CA, USA). Antibodies for immunohistochemistry and immunofluorescence were obtained from Abcam (Cambridge, MA, USA) unless indicated otherwise. Total RNA was isolated from total liver tissues, purified cholangiocytes, and selected cell lines using the TRI reagent from Sigma Life Science and reverse transcribed with the Reaction Ready First Strand cDNA Synthesis Kit (SABiosciences, Frederick, MD, USA) as described.²⁷ Total RNA was extracted from HSCs (isolated by laser capture microdissection, LMD) using the Arcturus PicoPure RNA Isolation Kit (Applied Biosystems, Waltham, MA, USA) according to the manufacturer's protocol.

The selected primers were purchased from Qiagen (Valencia, CA, USA). The following primers were used: miR-21, mouse-MS00011487; RNU6-6P, mouse-MS00033740; Bax, mouse-PPM02917E-200; cleaved caspase-3, mouse-PPM02922F-200; α -smooth muscle actin (α -SMA), mouse-PPM04483A-200; proliferating cell nuclear antigen (PCNA), mouse-PPM03456F-200; TGF- β 1, mouse-PPM02991B-200; matrix metalloproteinase-9 (MMP-9), mouse-PPM03661C-200; Smad-7, mouse-PPM03073F-200; and glyceraldehyde 3-phosphate dehydrogenase, mouse-PPM02946E-200.

Animal Models

All animal procedures were performed according to protocols approved by the Baylor Scott & White Health IACUC Committee. miR-21 knockout (miR-21^{-/-}) mice and background-matched miR-21^{+/+} (wild-type, WT), strain B6; 129) mice were purchased from Jackson Laboratory (Sacramento, CA, USA); the breeding colony is established in our animal facility. No gross defects or phenotypical changes are noted in the miR-21^{-/-} mice.²⁶ Male FVB/NJ WT mice

(control for Mdr2^{-/-} mice) were purchased from Jackson Laboratory. The breeding colony for Mdr2^{-/-} mice (purchased from Jackson Laboratory), a model of PSC,²⁸ is established in our animal facility. Animals were maintained in microisolator cages in a temperature-controlled environment with 12:12-h light–dark cycles; all animals were fed *ad libitum* a standard chow diet with free access to drinking water. Studies were performed in 12-week-old male miR-21^{-/-} mice (25–30 g) and their corresponding WT mice that were subjected to Sham or BDL for 1 week,^{16,29} and in 12-week-old male Mdr2^{-/-} mice (25–30 g) and their corresponding WT. Liver tissue samples and blocks (paraffin and frozen), serum, cholangiocytes, and cholangiocyte supernatants (after incubation at 37 °C for 4 h) were collected as described.^{2,29}

Isolated Cholangiocytes and HSCs, and Cell Lines

Virtually pure cholangiocytes were obtained by immunoaffinity separation^{2,6} by using a monoclonal antibody, rat IgG_{2a} (a gift from Dr. R. Faris, Brown University, Providence, RI, USA), against an unidentified antigen expressed by all mouse cholangiocytes. Cholangiocytes were isolated from three different groups of animals (each group consisted of 4 animals for a total of 12 mice). For each cholangiocyte preparation, we used four mice because of the low yield obtained with one single animal. Following cholangiocyte isolation, ~10 million cholangiocytes were incubated at 37 °C with 1 ml of HBS containing CaCl₂ for 4 h before supernatants were collected.

Activated HSCs were isolated from frozen liver tissue samples by LMD using the Leica LMD7000 (Leica Biosystems, Buffalo Grove, IL, USA) located at the Temple Health and Bioscience District (Temple, TX, USA). OCT-frozen liver sections (10 μ m) were fixed to glass foiled polyethylene naphthalate membrane slides and immunofluorescence for synaptophysin-9 (SYP-9, a marker of activated HSCs)³⁰ was performed to visualize activated HSCs. Fluorescently labeled, activated HSCs were manually separated from unwanted cells using an ultraviolet laser. Microdissected HSCs were then collected into PCR tubes and RNA was isolated using the Arcturus PicoPure RNA Isolation Kit (Applied Biosystems) according to the manufacturer's protocol.

The *in vitro* experiments were performed in our immortalized murine biliary cell line (IMCL)³¹ (a gift from Dr. Yoshiyuki Ueno, Yamagata University, Yamagata, Japan) as well as in our human hepatic stellate cell line (hHSC) that was purchased from ScienCell Research Laboratories (Carlsbad, CA, USA). IMCLs and hHSCs were maintained at standard conditions. IMCLs and hHSCs were treated with either 75 nM of *mirVana* miR-21 inhibitor or negative control (Thermo Fisher Scientific, Austin, TX, USA) for 48 h according to the manufacturer's protocol before cell pellets were collected. The miR-21 inhibitor contains a sequence that is 100% complementary to the sequence of active miR-21; therefore, binding between the inhibitor and miR-21 should be highly specific. As well, we have previously shown that use of this inhibitor *in vitro* is able to increase hepatocyte and HSC

expression of DR5 and Fas ligand, known targets of miR-21, by ~2-fold.²⁶ Unfortunately, as the inhibitor only binds to activated forms of miR-21 we are unable to detect accurately miR-21 expression levels as you may still get signals from the gene encoding miR-21, pri-miR-21, and pre-miR-21. For this reason, we based the specificity of our inhibitor on the expression of Bcl-2, a downstream target, in IMCL and hHSC (see Supplementary Figure 1).

Evaluation of miR-21 Expression

Isolation of miRNAs was performed in total liver and isolated cholangiocytes using the Ambion *mirVana* miRNA Isolation Kit from Life Technologies (Thermo Fischer Scientific, Waltham, MA, USA). Single-stranded cDNA was synthesized from 1 μ g of RNA from the aforementioned samples using the TaqMan microRNA Reverse Transcription Kit (Applied Biosystems) and was amplified by quantitative PCR (qPCR) using sequence-specific primers from the TaqMan microRNA Assays on an Applied Biosystems Vii7 Real-Time PCR System (Thermo Fisher Scientific) according to the manufacturer's protocol. The threshold cycle (C_T) is defined as the fractional cycle number at which the fluorescence passes the fixed threshold.

Control and late-stage PSC patient samples ($n=1$ each) were obtained from Dr Invernizzi under a protocol approved by the ethics committee by the Humanitas Research Hospital (Rozzano, Italy); the protocol was reviewed by the Veterans' Administration IRB and R&D committee. The protocol was approved by the Texas A&M HSC Institutional Review Board. Total RNA was extracted from formalin-fixed, paraffin-embedded sections from samples obtained from one control and one PSC patients using the RNeasy FFPE Kit (Qiagen, Valencia, CA, USA). From these samples, miR-21 expression was evaluated as described above.

Assessment of Liver Morphology, Serum Chemistry, Intrahepatic Bile Duct Mass, and Biliary Proliferation

Hematoxylin and eosin (H&E) staining was performed in paraffin-embedded liver sections (4–5 μ m, 10 different fields analyzed from each sample from three different animals). H&E-stained liver sections were evaluated by a board-certified pathologist to determine the degree of lobular damage, hepatic necrosis, and portal inflammation.

The serum levels of alanine transaminase (ALT) and alkaline phosphatase (ALP) were measured in Sham WT, BDL WT, Sham miR-21^{-/-}, and BDL miR-21^{-/-} mice by a

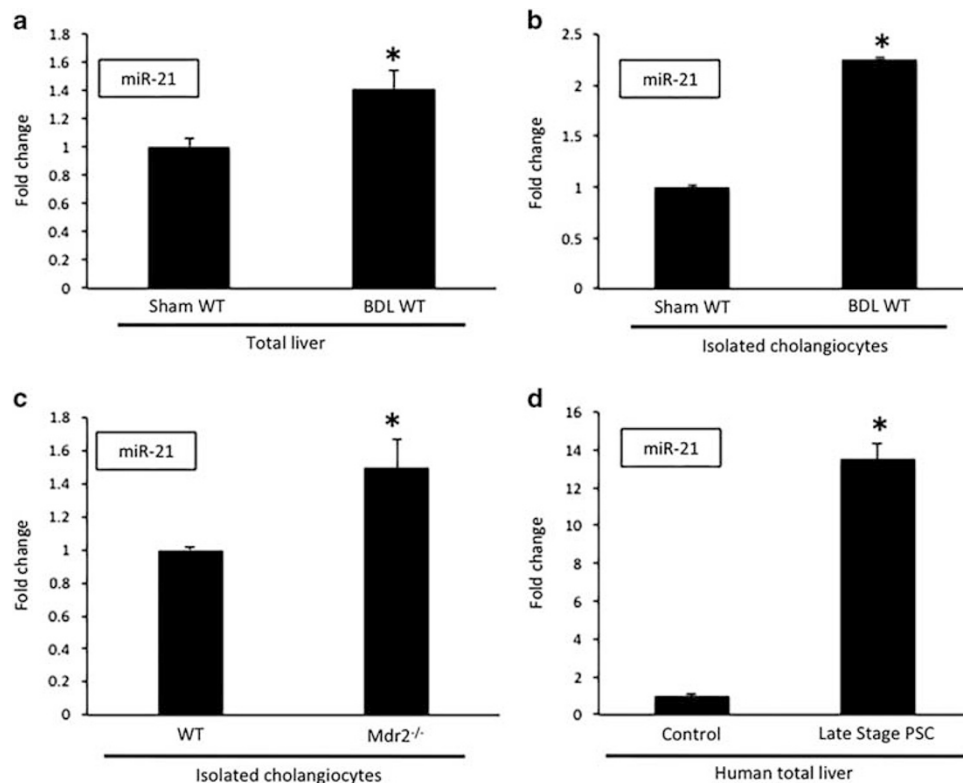


Figure 1 Evaluation of microRNA-21 (miR-21) expression following bile duct ligation (BDL). Following BDL, miR-21 levels are increased in total liver and isolated cholangiocytes (a and b). In Mdr2^{-/-} mice cholangiocytes have increased miR-21 expression (c). Total liver samples from primary sclerosing cholangitis (PSC) patients have increased miR-21 levels compared with normal patient samples (d). Data are expressed as means \pm s.e.m. $n=10$ reactions in total RNA collected from total liver and cholangiocytes from eight animals per group for quantitative PCR (qPCR). $n=3$ reactions per sample in total RNA collected from total liver from one human control and one human PSC sample. * $P<0.05$ versus Sham wild-type (WT), WT, human control.

Dimension RxL Max Integrated Chemistry system (Dade Behring, Deerfield, IL, USA) by the Chemistry Department, Baylor Scott & White Healthcare.

Intrahepatic bile duct mass (IBDM) was evaluated by semiquantitative immunohistochemistry for cytokeratin-19 (CK-19, a cholangiocyte specific marker).³² Biliary proliferation was evaluated in formalin-fixed, paraffin-embedded liver sections (4–5 μ m, 10 different fields analyzed from each sample from three different animals) by semiquantitative immunohistochemistry for Ki-67.³³ We used qPCR to analyze PCNA, Bax, and cleaved caspase-3 gene expression in RNA isolated from total liver, hHSC, and IMCL. qPCR was performed using RT² SYBR Green/ROX qPCR master mix for the Applied Biosystems ViiA7 qPCR system (Thermo

Fisher Scientific) according to the manufacturer's protocol. The comparative C_T method ($\Delta\Delta C_T$) was used for quantification of gene expression.

The proliferative rate of IMCL and hHSC was measured using the CellTiter 96 Aqueous Assay Kit (Promega, Madison, WI, USA). Transfected cells (10 000 per well) were plated in 96-well plates (BD Biosciences) and incubated at 37 °C, and cell proliferation was assessed after 48 h as described.⁷

Determination of Fibrosis, HSC Activation, and Smad-7 Expression

The fibrotic reaction was evaluated by qPCR for α -SMA, TGF- β 1, and collagen-1a expression in total RNA extracted from total liver tissue, LMD-isolated HSCs, and hHSC as

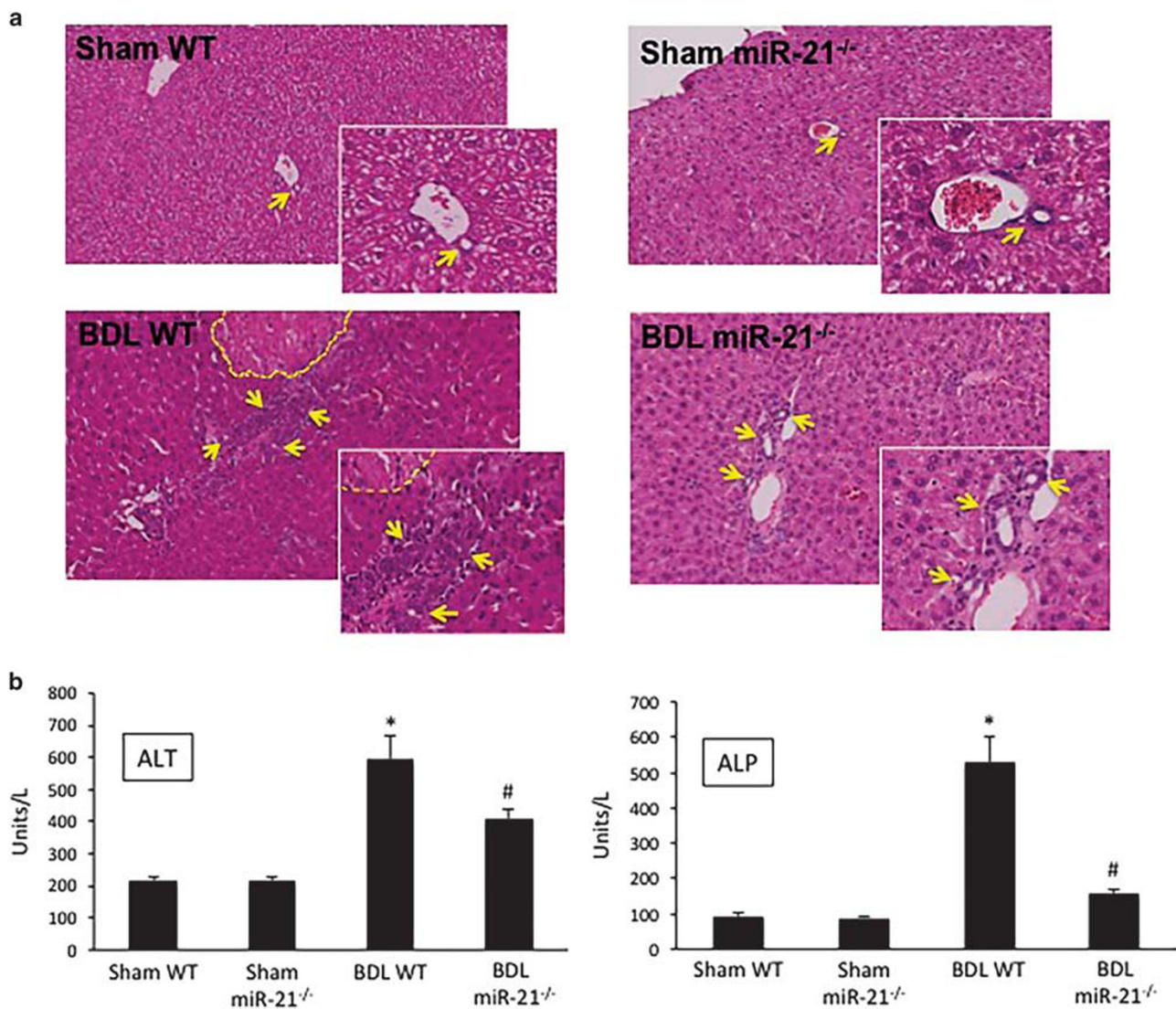


Figure 2 Assessment of liver injury. Loss of microRNA-21 (miR-21) ameliorates bile duct ligation (BDL)-induced necrosis, lobular damage, and portal inflammation as indicated by hematoxylin and eosin (H&E) staining (a). Yellow dashed line indicates areas of necrosis, whereas the yellow arrows point to bile ducts (a). BDL wild-type (WT) mice show increased serum levels of alanine transaminase (ALT) and alkaline phosphatase (ALP) when compared with BDL WT; however, these parameters are decreased in BDL miR-21^{-/-} mice when compared with BDL WT mice (b). Data are expressed as means \pm s.e.m. $n=3$ reactions in serum collected from eight animals each per animal group for serum chemistry. * $P<0.05$ versus Sham WT; # $P<0.05$ versus BDL WT. Representative images are shown for H&E. Original magnification, $\times 20$.

described above. Collagen deposition was visualized in liver sections using Sirius Red staining as described.⁷ Activation of HSCs was visualized in liver sections by immunofluorescent staining for either SYP-9 or α -SMA, which was costained with CK-19 (only expressed by cholangiocytes) to visualize intrahepatic bile ducts.

The role of cholangiocyte-derived factors on HSC activation was determined by incubating hHSCs *in vitro* with cholangiocyte supernatants from Sham WT, Sham miR-21^{-/-}, BDL WT, or BDL miR-21^{-/-} mice for 48 h. Fibrosis gene expression was determined by qPCR for FN-1 and collagen-1a.

As miR-21 has been shown to bind Smad-7 during an experimental model of non-alcoholic steatohepatitis,²⁵ we

measured in total liver and isolated cholangiocytes the expression of Smad-7 by qPCR.

Statistical Analysis

Data are expressed as mean \pm s.e.m. Differences between groups were analyzed by the Student's unpaired *t*-test when two groups were analyzed, and by two-way ANOVA when more than two groups were analyzed.

RESULTS

miR-21 Expression is Increased During Cholestasis

Following BDL, there was a significant increase in miR-21 expression in total liver and isolated cholangiocytes when compared with Sham WT mice (Figure 1a and b). miR-21

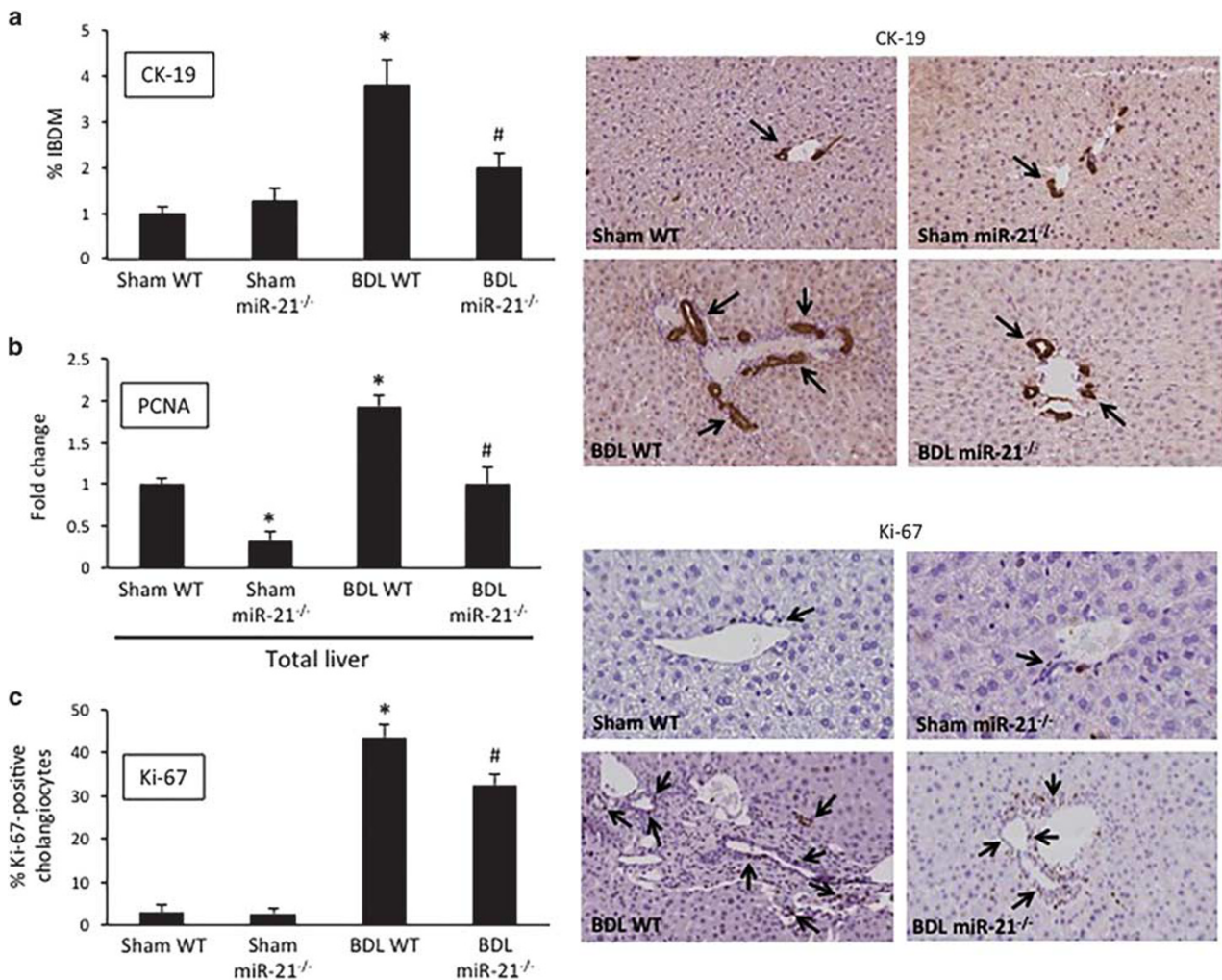


Figure 3 Measurement of intrahepatic bile duct mass (IBDM) and biliary proliferation. Following bile duct ligation (BDL), there is increased IBDM compared with Sham wild-type (WT) (a). The loss of microRNA-21 (miR-21) reduces the degree BDL-induced IBDM compared with BDL WT (a). Following BDL, mice have increased levels of proliferating cell nuclear antigen (PCNA), which is significantly decreased in BDL miR-21^{-/-} mice compared with BDL WT (b). Immunohistochemistry and semiquantitative analysis are shown for the proliferative marker Ki-67 (c). There is increased biliary Ki-67 expression in BDL WT compared with Sham WT, but the loss of miR-21 decreases BDL-induced biliary Ki-67 expression (c). Data are expressed as means \pm s.e.m. *n* = 7 reactions in total RNA collected from eight animals per group for quantitative PCR (qPCR), *n* = 10 pictures from six animals per group for immunohistochemistry. **P* < 0.05 versus Sham WT; #*P* < 0.05 versus BDL WT. Representative images are shown for cytokeratin-19 (CK-19) and Ki-67 immunohistochemistry. Original magnification, \times 20.

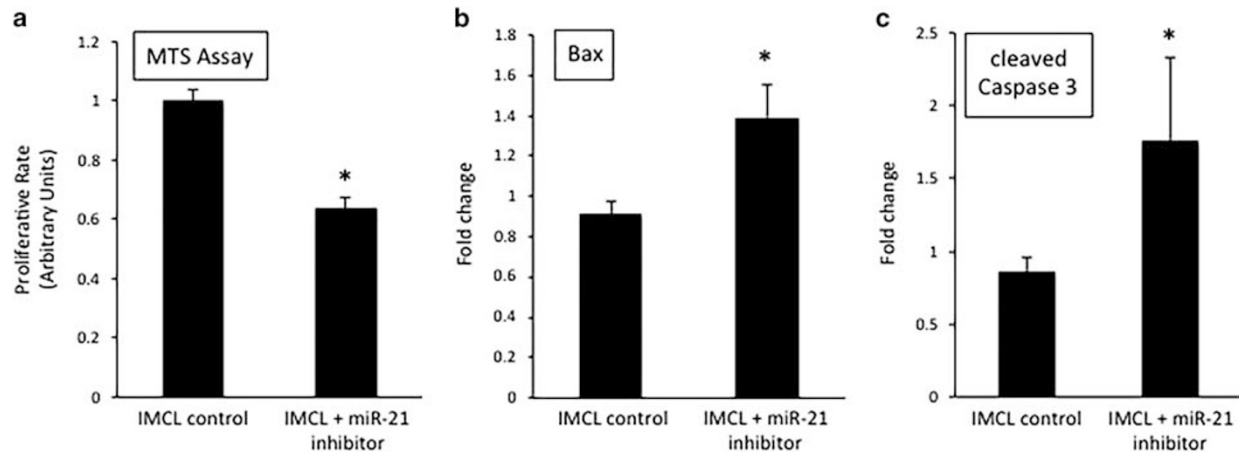


Figure 4 Evaluation of immortalized murine biliary cell lines (IMCL) proliferation and apoptosis. Following treatment with microRNA-21 (miR-21) inhibitor, IMCLs have decreased proliferation, as shown by MTS assay, and increased Bax and cleaved caspase-3 gene expression when compared with control treated (a–c). Data are expressed as mean \pm s.e.m. $n=6$ reactions in total RNA from 12 sets of cells for quantitative PCR (qPCR), $n=10$ experiments per group for MTS assay. * $P<0.05$ versus IMCL control.

expression was also increased in cholangiocytes from *Mdr2*^{-/-} mice³⁴ when compared with the corresponding WT mice, as well as in total liver extracted from a late-stage PSC patient when compared with a normal liver sample. These findings suggest that during cholestatic injury, such as BDL or PSC, miR-21 levels are increased and may contribute to the progression of biliary injury and hepatic fibrosis.

Loss of miR-21 Ameliorates Liver Damage

Following BDL, there was moderate portal inflammation, ductal proliferation, and multifocal areas of necrosis when compared with Sham WT mice; however, the amount of damage observed in BDL miR-21^{-/-} mice was greatly decreased when compared with BDL WT mice, suggesting that miR-21 promotes liver damage during cholestatic injury (Figure 2a). No significant changes were noted in Sham miR-21^{-/-} mice compared with Sham WT mice (Figure 2a). Similarly, the levels of the liver enzymes ALT and ALP were increased in serum from BDL WT compared with Sham WT mice; however, ALT and ALP serum levels were decreased in BDL miR-21^{-/-} mice compared with BDL WT mice (Figure 2b). These studies indicate that the loss of miR-21 during BDL-induced cholestatic injury ameliorates liver damage associated with this injury.

Knockout of miR-21 Decreases BDL-Induced IBDM and Biliary Proliferation

Consistent with previous findings,³⁵ following BDL there was a significant increase in IBDM when compared with Sham WT mice, which was reduced in BDL miR-21^{-/-} compared with BDL WT mice (Figure 3a). No significant changes in IBDM were noted in Sham miR-21^{-/-} mice when compared with Sham WT mice (Figure 3a). As shown by qPCR in total liver samples, BDL WT mice have increased PCNA expression when compared with Sham WT; however, there was

decreased PCNA expression in Sham miR-21^{-/-} and BDL miR-21^{-/-} mice when compared with Sham WT and BDL WT, respectively (Figure 3b). Furthermore, the biliary expression of Ki-67 was increased in BDL WT mice compared with Sham WT, which was significantly decreased in BDL miR-21^{-/-} mice when compared with BDL WT mice (Figure 3c). No significant changes were noted in the biliary expression of Ki-67 in Sham miR-21^{-/-} mice when compared with Sham WT mice (Figure 3c). These findings demonstrate that during cholestasis the loss of miR-21 reduces IBDM and biliary proliferation associated with this injury.

Inhibition of miR-21 Decreases Cholangiocyte Proliferation In Vitro

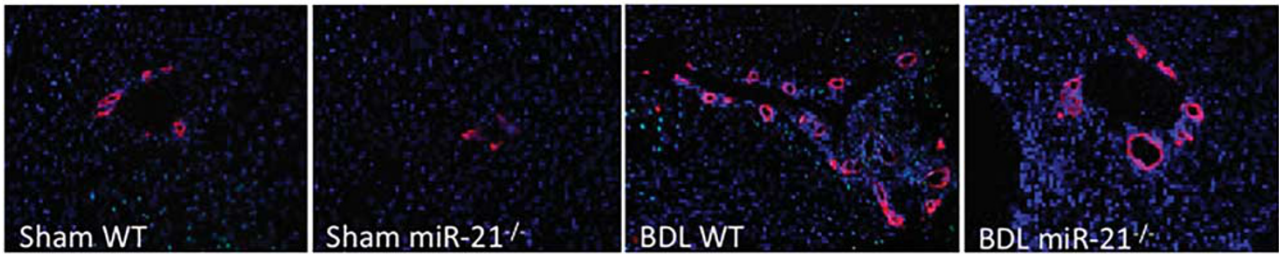
In vitro, IMCL treated with miR-21 inhibitor had decreased proliferative capacity when compared with IMCL treated with control (Figure 4a). Consequently, IMCL that were treated with miR-21 inhibitor had increased expression of the apoptotic factors Bax and cleaved caspase-3 (Figure 4b and c) when compared with control treated cells. These data indicate that inhibition of miR-21 in cholangiocytes leads to decreased proliferation and increased apoptosis *in vitro*.

Loss of miR-21 Decreases BDL-Induced HSC Activation and Fibrotic Reaction

As the activation of HSCs is known to be a key player in the development of fibrosis,³⁶ we analyzed HSC activation *in vivo* by staining for SYP-9 or α -SMA (markers of activated HSCs) and CK-19 (to visualize bile ducts) in liver sections by immunofluorescence. The expression of SYP-9 and CK-19 seemed unchanged between Sham WT and Sham miR-21^{-/-} mice; however, the number of SYP-9-positive cells was increased in BDL WT, which was accompanied with increased IBDM. In BDL miR-21^{-/-} mice the number of SYP-9-positive cells was decreased compared with BDL WT, and this

a

Syp-9 / CK-19 / DAPI



b

α -SMA / CK-19 / DAPI

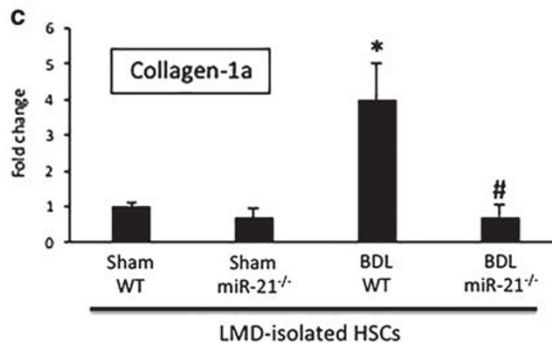
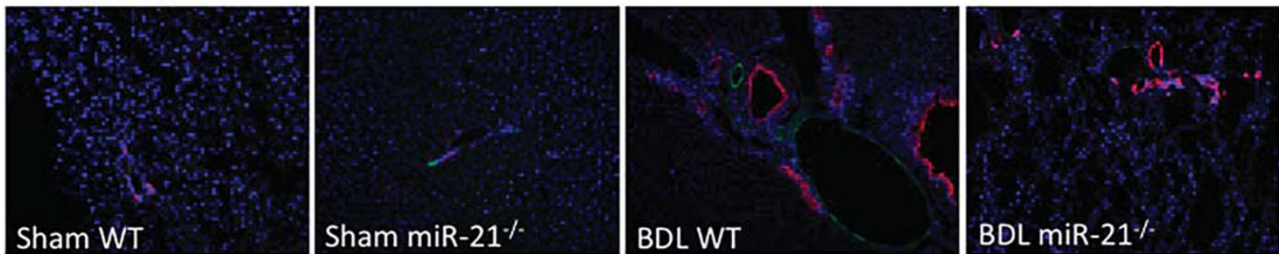


Figure 5 Evaluation of hepatic stellate cell (HSC) activation and fibrotic reaction. As shown by immunofluorescence co-stain for synaptophysin-9 (SYP-9) (green) and cytokeratin-19 (CK-19) (red), there is increased HSC activation and intrahepatic bile duct mass (IBDM) in bile duct ligation wild-type (BDL WT) compared with Sham WT, but this is decreased in BDL miR-21^{-/-} mice when compared with BDL WT, respectively (a). Immunofluorescent costain for α -smooth muscle actin (α -SMA) (green) and CK-19 (red) show increased HSC activation and IBDM in BDL WT compared with Sham WT, but this is decreased in BDL miR-21^{-/-} when compared with BDL WT (b). In HSCs that are isolated from BDL WT, there is a significant increase in collagen-1a expression when compared with HSCs isolated from Sham WT; however, collagen-1a expression is significantly decreased in HSCs isolated from BDL miR-21^{-/-} when compared with HSCs isolated from BDL WT (c). Data are expressed as means \pm s.e.m. $n=6$ reactions in total RNA from six animals per group for quantitative PCR (qPCR). * $P<0.05$ versus Sham WT; # $P<0.05$ versus BDL WT. Representative images are shown for SYP-9 and CK-19 immunofluorescence. Original magnification, $\times 20$.

was also accompanied by decreased IBDM (Figure 5a). Staining for α -SMA and CK-19 showed the same trend as the SYP-9 staining (Figure 5b). Recently, studies have indicated that miR-21 has a profibrotic role during models of drug-induced cholestasis, and that inhibition of miR-21 can ameliorate this damage.^{37,38} In HSCs that were isolated from BDL WT, we see increased expression of collagen-1a when compared with Sham WT (Figure 5c). In contrast, in HSCs that were isolated from BDL miR-21^{-/-} these parameters are decreased when compared with BDL WT (Figure 5c). No significant differences were noted between HSCs isolated from Sham WT and Sham miR-21^{-/-}. These

data further imply that increased miR-21 levels can contribute to increased fibrosis via HSC activation and fibrotic reaction.

Knockout of miR-21 Reduces the Amount of BDL-Associated Fibrosis

Next, we aimed to explore the role of miR-21 during BDL-induced fibrosis.²⁵ In total liver samples, we found that the expression of α -SMA and TGF- β 1 was significantly increased in BDL WT compared with Sham WT mice, but was significantly decreased in the livers of BDL miR-21^{-/-} compared with BDL WT mice (Figure 6a and b). Furthermore, collagen deposition was increased in the livers of BDL

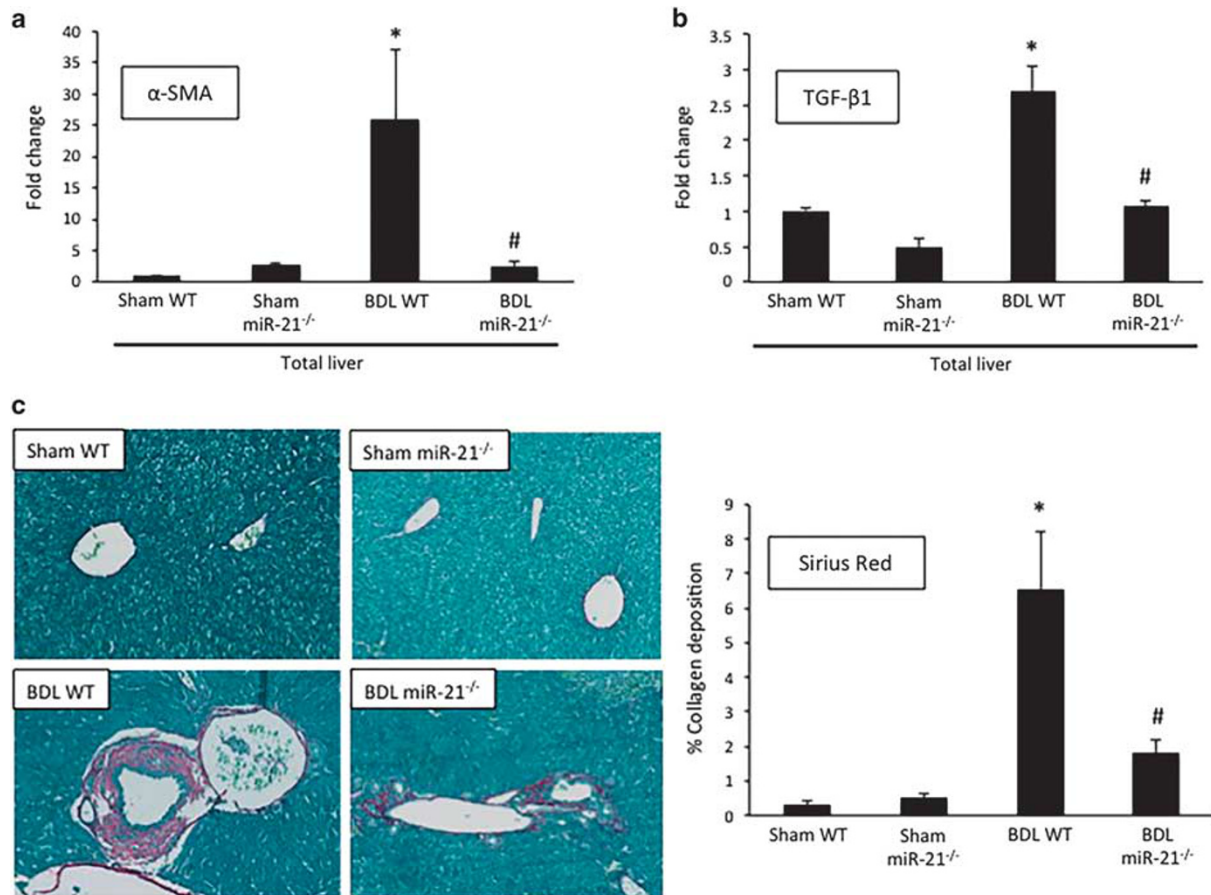


Figure 6 Determination of fibrotic reaction. In bile duct ligation wild-type (BDL WT), there is a significant increase in α -smooth muscle actin (α -SMA) and transforming growth factor- β 1 (TGF- β 1) gene expression compared with Sham WT; however, this is significantly decreased in BDL miR-21^{-/-} when compared with BDL WT (a and b). Collagen deposition is significantly increased following BDL when compared with Sham WT; however, the loss of microRNA-21 (miR-21) blunts this effect (c). Data are expressed as means \pm s.e.m., $n=6$ reactions in total RNA from eight animals per group for quantitative PCR (qPCR), $n=20$ pictures from six animals used for Sirius Red staining. * $P<0.05$ versus WT; # $P<0.05$ versus BDL WT. Representative images are shown for Sirius Red staining. Original magnification, $\times 20$.

WT mice compared with Sham WT mice, but was significantly decreased in the livers of BDL miR-21^{-/-} mice when compared with BDL WT mice (Figure 6c). There was no significant difference between the expression of α -SMA and TGF- β 1, and collagen deposition in the livers of Sham WT and Sham miR-21^{-/-} mice. These findings, along with the above data indicating that miR-21 promotes HSC activation, suggest that the loss of miR-21 during cholestatic injury decreases the associated fibrotic reaction.

Inhibition of miR-21 Decreases HSC Proliferation and Fibrotic Reaction *In Vitro*

As demonstrated above, miR-21 seems to have a role in HSC activation and proliferation following BDL *in vivo* (Figure 5). To further validate these findings, we took hHSCs and treated them with either miR-21 inhibitor or control. Following treatment, proliferative capacity was decreased in hHSC treated with a miR-21 inhibitor when compared with hHSC treated with control as demonstrated by MTS assay and

PCNA expression (Figure 7a and b). Concomitantly, hHSCs treated with miR-21 inhibitor have increased Bax expression when compared with control treated cells (Figure 7c), indicating that the loss of miR-21 decreases HSC proliferation. We wanted to look further at the role of miR-21 during HSC activation as we previously noted that BDL miR-21^{-/-} mice have decreased HSC activation when compared with BDL WT mice (Figure 5). By qPCR, we found that hHSCs treated with miR-21 inhibitor had decreased expression of α -SMA when compared with control (Figure 7d). These findings suggest that the loss of miR-21 decreases the degree of HSC proliferation and fibrotic reaction, which could be an important target to halt cholestasis-induced hepatic fibrosis progression.

Loss of miR-21 Increases Smad-7 Expression *In Vivo*

Smad-7 has been reported as a target of miR-21,²⁵ and as Smad signaling is involved in the promotion of hepatic fibrosis in both cholangiocytes and HSCs during models of

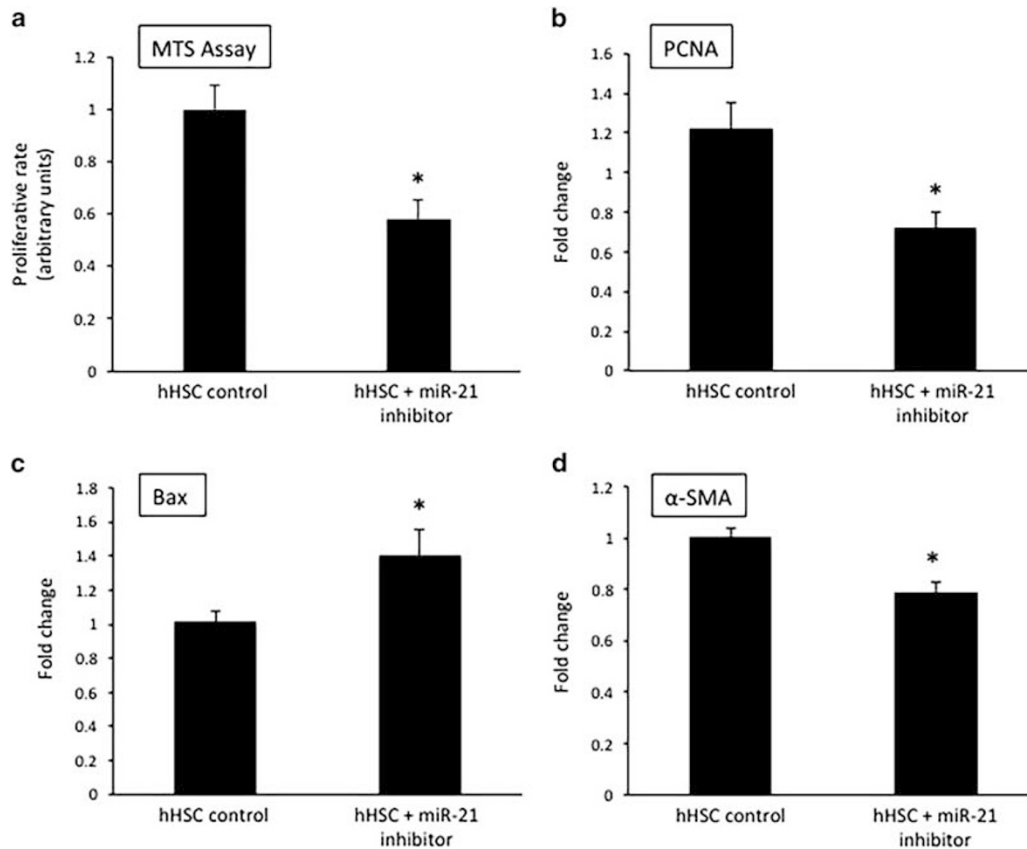


Figure 7 Evaluation of human hepatic stellate cell line (hHSC) proliferation, apoptosis and fibrotic reaction, *in vitro*. hHSCs treated with miR-21 inhibitor have decreased proliferation, increased Bax, and decreased α -smooth muscle actin (α -SMA) and matrix metalloproteinase-9 (MMP-9) gene expression when compared with control treated (a–d). Data are expressed as means \pm s.e.m.; $n = 6$ reactions from 12 sets of cells for quantitative PCR (qPCR), $n = 10$ experiments for MTS assay. * $P < 0.05$ versus hHSC control.

cholestasis,^{16,36} we evaluated the expression of Smad-7 in our model. In BDL WT mice, there was no significant change in the expression of Smad-7 in both total liver and isolated cholangiocytes when compared with Sham WT (Figure 8a and b); however, Sham and BDL miR-21^{-/-} mice showed increased Smad-7 when compared with Sham and BDL WT, respectively (Figure 8a and b). These data demonstrate that miR-21 can regulate Smad-7 within cholangiocytes during cholestasis.

HSCs Treated with Supernatants from Cholangiocytes Lacking miR-21 have Decreased Fibrotic Reaction *In Vitro*

We next evaluated the effect of cholangiocyte supernatant from Sham and BDL WT and miR-21^{-/-} mice (that do not contain miR-21) on HSC activation. We incubated hHSCs with supernatants from cholangiocytes isolated from Sham WT, BDL WT, Sham miR-21^{-/-}, and BDL miR-21^{-/-} animals. There was increased FN-1 and collagen-1a expression in hHSCs treated with cholangiocyte supernatants from BDL WT when compared with supernatant from Sham WT mice; however, these factors were decreased in hHSCs treated with cholangiocyte supernatants from BDL miR-21^{-/-}

animals compared with supernatant from BDL WT mice (Figure 9a and b). These data imply that cholangiocyte signaling strongly impacts HSC activation during cholestatic injury, and these profibrotic factors may be regulated by miR-21.

DISCUSSION

To summarize these findings, in the BDL and Mdr2^{-/-} cholestatic models miR-21 is upregulated in total liver and cholangiocytes. We have also shown that human PSC sample has increased miR-21 levels when compared with normal liver. Within cholangiocytes and HSCs, miR-21 promotes proliferation and fibrosis, and decreases apoptosis. Once activated, HSCs are able to secrete fibrosis-promoting factors that lead to increased hepatic damage. We demonstrated that miR-21 regulates HSC activation and Smad signaling, which in turn stimulates fibrogenesis. Loss of miR-21 leads to decreased biliary hyperplasia, HSC activation, and fibrosis that are associated with BDL.

Studies have shown that the expression of miR-21 (that is ubiquitously expressed throughout the body)^{38,39} is increased in cholangiocarcinoma (CCA) tissue when compared with

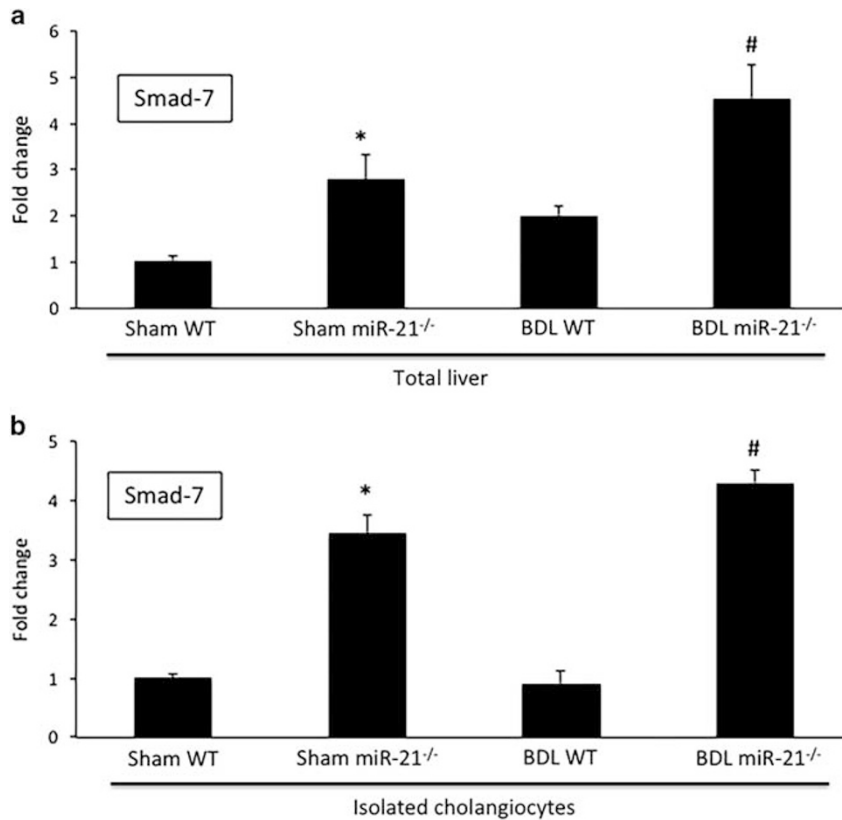


Figure 8 Evaluation of small mothers against decapentaplegic 7 (Smad-7) expression. In total liver and isolated cholangiocytes from bile duct ligation wild-type (BDL WT) mice, there is increased decreased Smad-7, as shown by quantitative PCR (qPCR), when compared with Sham WT (**a** and **b**). However, total liver and isolated cholangiocytes from BDL miR-21^{-/-} mice show increased Smad-7 when compared with BDL WT (**a** and **b**); $n=9$ reactions from total RNA from six animals for qPCR. * $P<0.05$ vs Sham WT; # $P<0.05$ vs BDL WT.

normal biliary epithelium.^{40,41} We found that hepatic miR-21 levels are significantly increased in PSC when compared with control samples. As chronic cholestasis can be a risk factor for developing CCA, it is important to understand the role of miR-21 during liver injury.

Previous studies have shown that miR-21 is upregulated during models of chronic liver injury, inhibits apoptosis, and regulates cell survival.^{25,26} Increased miR-21 levels are commonly noted during cell proliferation and stress;⁴² however, it remains controversial as to which liver cell type is targeted by miR-21.^{43,44} Here we show that miR-21 expression is upregulated in cholangiocytes following BDL and in the *Mdr2*^{-/-} model of PSC. Furthermore, the loss of miR-21 reduced the BDL-induced cholangiocyte proliferation compared with BDL WT mice. This is further highlighted where we show that treatment of IMCL with a miR-21 inhibitor leads to decreased proliferative activity, with a concomitant increase in apoptosis.

With regard to the possible target cells of the miR-21 inhibitor in our *in vivo* models, we propose that cholangiocytes and HSCs are two important target cells of the miR-21 inhibitor. In support of this, in the *in vitro* studies we determined that cholangiocytes and HSCs contain miR-21,

and treatment with the miR-21 inhibitor impacted growth and activation in these cell types. However, *in vivo* we used a miR-21^{-/-} mouse model, resulting in complete loss of miR-21 in all cells. Further *in vivo* studies are needed to pinpoint the target cells of the miR-21 inhibitor in normal and cholestatic models.

Currently, there is limited data regarding the role of miR-21 in HSCs during hepatic fibrosis, and no current literature exists regarding its role in cholangiocytes during cholestasis. One study found that HSCs containing miR-21 promote their own activation during injury;^{37,38} however, existing publications do not consistently report on miR-21 levels in activated HSCs.^{44,45} Our findings indicate that mice lacking miR-21 have decreased HSC activation when compared with BDL WT mice. On the basis of our findings, we propose that HSC activation is regulated by miR-21 during cholestatic injury, and activation can be further maintained by protecting the activated HSCs from apoptosis.

Previous work has shown that Smad signaling can influence HSC activation and cholangiocyte proliferation during models of cholestatic injury.^{16,36} Here we show that loss of miR-21 increases Smad-7 expression in both total liver and isolated cholangiocytes. These findings provide evidence that

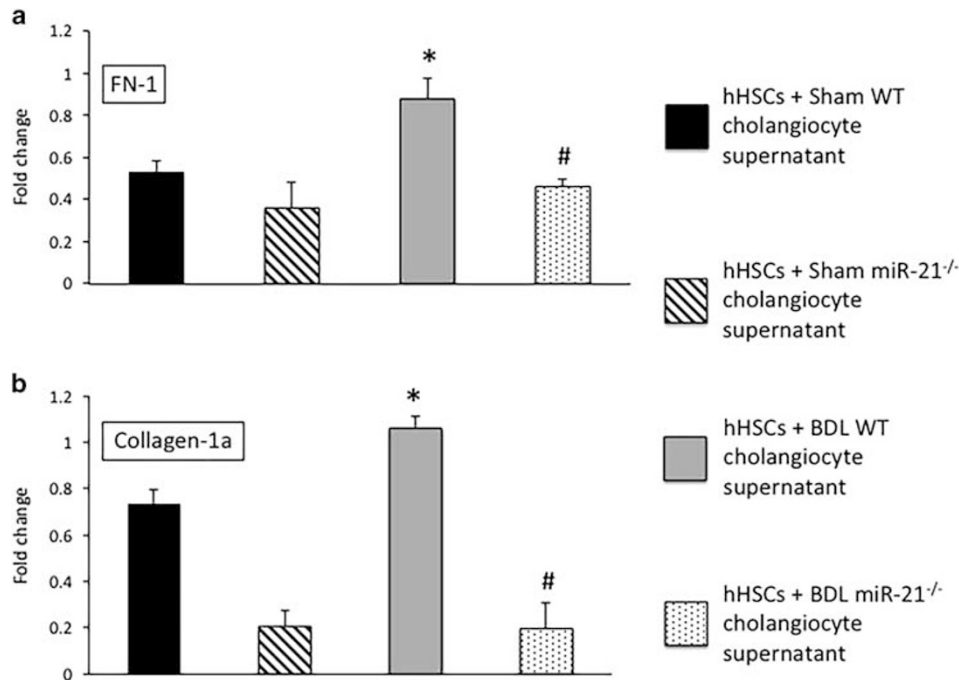


Figure 9 Determination of human hepatic stellate cell line (hHSC) fibrotic reaction, *in vitro*. hHSCs treated with supernatants extracted from cholangiocytes isolated from bile duct ligation wild-type (BDL WT) mice show increased FN-1, and collagen-1a expression when compared with hHSCs treated with supernatants from Sham WT mice (**a** and **b**); however, these parameters were decreased in hHSCs treated with cholangiocyte supernatants from BDL miR-21^{-/-} mice when compared with BDL WT mice (**a** and **b**). Data are expressed as means \pm s.e.m. $n=6$ reactions from 12 sets of cells for qPCR. * $P<0.05$ versus hHSCs+WT cholangiocyte supernatants; # $P<0.05$ versus hHSCs+BDL WT cholangiocyte supernatants.

miR-21 increases fibrogenesis during hepatic injury by inhibiting the inhibitory Smad-7.

It is known that many hepatic cell types can interact and signal to one another via paracrine mediators to influence disease progression. Specifically, it has been noted that cholangiocytes can signal to HSCs to regulate their activation.^{46,47} Our data indicate that hHSCs treated with supernatant isolated from cholangiocytes lacking miR-21 have decreased fibrotic reaction, further verifying that cholangiocyte-secreted factors can influence HSC response during cholestatic injury. Previously, it has been shown that the lumen of intrahepatic bile ducts of cystic liver contains exosome-like vesicles, and these exosomes are cholangiocyte-derived.⁴⁸ As well, rats that undergo partial hepatectomy show increased serum levels of exosome-like vesicles containing miR-21 when compared with normal rats.⁴⁹ Based on this work, we hypothesize that during cholestatic injury cholangiocytes may secrete exosomes containing miR-21 that can increase HSC activation.

Our data shed further light on the impact that miR-21 has on hepatic fibrosis, specifically in the realm of cholestatic injury. It has been proposed that miR-21 is strongly upregulated in HSCs during thioacetamide- and carbon tetrachloride-induced hepatic fibrosis.³⁸ These studies along with our findings promote the idea that miR-21 regulates hepatic fibrosis through the modulation of HSC activation and proliferation. Aside from hepatic fibrosis, we provide

evidence that miR-21 (i) is upregulated in cholangiocytes following injury, (ii) enhances cholangiocyte proliferation, and (iii) hinders cholangiocyte apoptotic processes. Increased HSC activation and cholangiocyte proliferation may be driven by miR-21 regulation of Smad-7. In this regard, modulation of miR-21 during fibrosis-related hepatic injury may be useful. Further elucidation of the pathways that are modulated by miR-21 during these processes is essential to uncovering therapeutic targets.

Supplementary Information accompanies the paper on the Laboratory Investigation website (<http://www.laboratoryinvestigation.org>)

ACKNOWLEDGMENTS

We would like to gratefully acknowledge the Temple Health and Bioscience Economic Development District for allowing us to use their Leica LMD7000 for HSC isolation. This work was supported, in part, by the Dr Nicholas C Hightower Centennial Chair of Gastroenterology from Scott & White, a VA Research Career Scientist Award, a VA Merit award to Dr Alpini (5I01BX000574), a VA Merit Award (1I01BX003031) to Dr Francis, a VA Merit Award (5I01BX002192) to Dr Glaser, and a VA Merit Award (1I01BX001724) to Dr Meng from the United States (US) Department of Veterans Affairs Biomedical Laboratory Research, a NIH Grant DK108959 to Dr Francis, and the NIH Grants DK058411, DK076898, DK107310, and DK062975 to Drs Alpini, Meng, and Glaser. This material is the result of work supported by resources at the Central Texas Veterans Health Care System. The views expressed in this article are those of the authors and do not necessarily represent the views of the Department of Veterans Affairs.

DISCLOSURE/CONFLICT OF INTEREST

The authors declare no conflict of interest.

- Renzi A, DeMorrow S, Onori P, *et al*. Modulation of the biliary expression of arylalkylamine N-acetyltransferase alters the autocrine proliferative responses of cholangiocytes in rats. *Hepatology* 2013;57:1130–1141.
- Glaser S, Meng F, Han Y, *et al*. Secretin stimulates biliary cell proliferation by regulating expression of microRNA 125b and microRNA let7a in mice. *Gastroenterology* 2014;146:1795–1808.
- Desmet VJ. Histopathology of cholestasis. *Verh Dtsch Ges Pathol* 1995;79:233–240.
- Li MK, Crawford JM. The pathology of cholestasis. *Semin Liv Dis* 2004;24:21–42.
- Alpini G, Lenzi R, Sarkozi L, *et al*. Biliary physiology in rats with bile ductular cell hyperplasia. Evidence for a secretory function of proliferated bile ductules. *J Clin Invest* 1988;81:569–578.
- Glaser S, Gaudio E, Rao A, *et al*. Morphological and functional heterogeneity of the mouse intrahepatic biliary epithelium. *Lab Invest* 2009;89:456–469.
- Han Y, Onori P, Meng F, *et al*. Prolonged exposure of cholestatic rats to complete dark inhibits biliary hyperplasia and liver fibrosis. *Am J Physiol Gastrointest Liver Physiol* 2014;307:G894–G904.
- Alpini G, Glaser S, Ueno Y, *et al*. Heterogeneity of the proliferative capacity of rat cholangiocytes after bile duct ligation. *Am J Physiol Gastrointest Liver Physiol* 1998;274:G767–G775.
- Alvaro D, Mancino MG, Glaser S, *et al*. Proliferating cholangiocytes: a neuroendocrine compartment in the diseased liver. *Gastroenterology* 2007;132:415–431.
- Maroni L, Haibo B, Ray D, *et al*. Functional and structural features of cholangiocytes in health and disease. *Cell Mol Gastroenterol Hepatol* 2015;1:368–380.
- Hall C, Sato K, Wu N, *et al*. Regulators of cholangiocyte proliferation. *Gene Expr* 2016 (E-pub ahead of print)
- Wells RG. Cellular sources of extracellular matrix in hepatic fibrosis. *Clin Liver Dis* 2008;12:759–768, viii.
- Friedman SL. Molecular regulation of hepatic fibrosis, an integrated cellular response to tissue injury. *J Biol Chem* 2000;275:2247–2250.
- Wallace K, Burt AD, Wright MC. Liver fibrosis. *Biochem J* 2008;411:1–18.
- Friedman SL. Hepatic fibrosis – overview. *Toxicology* 2008;254:120–129.
- Wu N, Meng F, Invernizzi P, *et al*. The secretin/secretin receptor axis modulates liver fibrosis through changes in TGF-beta1 biliary secretion. *Hepatology* 2016;64:865–879.
- Kerr TA, Korenblat KM, Davidson NO. MicroRNAs and liver disease. *Trans Res* 2011;157:241–252.
- Fabian MR, Sonenberg N, Filipowicz W. Regulation of mRNA translation and stability by microRNAs. *Annu Rev Biochem* 2010;79:351–379.
- Djuranovic S, Nahvi A, Green R. miRNA-mediated gene silencing by translational repression followed by mRNA deadenylation and decay. *Science* 2012;336:237–240.
- Alisi A, Da Sacco L, Bruscalupi G, *et al*. Mirnome analysis reveals novel molecular determinants in the pathogenesis of diet-induced nonalcoholic fatty liver disease. *Lab Invest* 2011;91:283–293.
- Pogribny IP, Starlard-Davenport A, Tryndyak VP, *et al*. Difference in expression of hepatic microRNAs miR-29c, miR-34a, miR-155, and miR-200b is associated with strain-specific susceptibility to dietary nonalcoholic steatohepatitis in mice. *Lab Invest* 2010;90:1437–1446.
- Murakami Y, Toyoda H, Tanaka M, *et al*. The progression of liver fibrosis is related with overexpression of the miR-199 and 200 families. *PLoS One* 2011;6:e16081.
- Meng F, Henson R, Wehbe-Janek H, *et al*. MicroRNA-21 regulates expression of the PTEN tumor suppressor gene in human hepatocellular cancer. *Gastroenterology* 2007;133:647–658.
- Chusorn P, Namwat N, Loilome W, *et al*. Overexpression of microRNA-21 regulating PDCD4 during tumorigenesis of liver fluke-associated cholangiocarcinoma contributes to tumor growth and metastasis. *Tumour Biol* 2013;34:1579–1588.
- Dattaroy D, Pourhoseini S, Das S, *et al*. Micro-RNA 21 inhibition of SMAD7 enhances fibrogenesis via leptin-mediated NADPH oxidase in experimental and human nonalcoholic steatohepatitis. *Am J Physiol Gastrointest Liver Physiol* 2015;308:G298–G312.
- Francis H, McDaniel K, Han Y, *et al*. Regulation of the extrinsic apoptotic pathway by microRNA-21 in alcoholic liver injury. *J Biol Chem* 2014;289:27526–27539.
- Venter J, Francis H, Meng F, *et al*. Development and functional characterization of extrahepatic cholangiocyte lines from normal rats. *Dig Liver Dis* 2015;47:964–972.
- de Vree JM, Jacquemin E, Sturm E, *et al*. Mutations in the MDR3 gene cause progressive familial intrahepatic cholestasis. *Proc Natl Acad Sci USA* 1998;95:282–287.
- Graf A, Meng F, Hargrove L, *et al*. Knockout of histidine decarboxylase decreases bile duct ligation-induced biliary hyperplasia via down-regulation of the histidine decarboxylase/VEGF axis through PKA-ERK1/2 signaling. *Am J Physiol Gastrointest Liver Physiol* 2014;307:G813–G823.
- Friedman SL. Hepatic stellate cells: protean, multifunctional, and enigmatic cells of the liver. *Physiol Rev* 2008;88:125–172.
- Kennedy LL, Hargrove LA, Graf AB, *et al*. Inhibition of mast cell-derived histamine secretion by cromolyn sodium treatment decreases biliary hyperplasia in cholestatic rodents. *Lab Invest* 2014;94:1406–1418.
- LeSage G, Glaser S, Gubba S, *et al*. Regrowth of the rat biliary tree after 70% partial hepatectomy is coupled to increased secretin-induced ductal secretion. *Gastroenterology* 1996;111:1633–1644.
- DeMorrow S, Meng F, Venter J, *et al*. Neuropeptide Y inhibits biliary hyperplasia of cholestatic rats by paracrine and autocrine mechanisms. *Am J Physiol Gastrointest Liver Physiol* 2013;305:G250–G257.
- Baghdasaryan A, Claudel T, Kusters A, *et al*. Curcumin improves sclerosing cholangitis in *Mdr2*^{-/-} mice by inhibition of cholangiocyte inflammatory response and portal myofibroblast proliferation. *Gut* 2010;59:521–530.
- Glaser S, Ueno Y, DeMorrow S, *et al*. Knockout of alpha-calcitonin gene-related peptide reduces cholangiocyte proliferation in bile duct ligated mice. *Lab Invest* 2007;87:914–926.
- Khanizadeh S, Ravanshad M, Hosseini S, *et al*. Blocking of SMAD4 expression by shRNA effectively inhibits fibrogenesis of human hepatic stellate cells. *Gastroenterol Hepatol Bed Bench* 2015;8:262–269.
- Wei J, Feng L, Li Z, *et al*. MicroRNA-21 activates hepatic stellate cells via PTEN/Akt signaling. *Biomed Pharmacother* 2013;67:387–392.
- Zhang Z, Gao Z, Hu W, *et al*. 3,3'-Diindolylmethane ameliorates experimental hepatic fibrosis via inhibiting miR-21 expression. *Br J Pharmacol* 2013;170:649–660.
- Sayed D, Rane S, Lypowy J, *et al*. MicroRNA-21 targets Sprouty2 and promotes cellular outgrowths. *Mol Biol Cell* 2008;19:3272–3282.
- Lu L, Byrnes K, Han C, *et al*. miR-21 targets 15-PGDH and promotes cholangiocarcinoma growth. *Mol Cancer Res* 2014;12:890–900.
- Wang LJ, He CC, Sui X, *et al*. MiR-21 promotes intrahepatic cholangiocarcinoma proliferation and growth *in vitro* and *in vivo* by targeting PTPN14 and PTEN. *Oncotarget* 2015;6:5932–5946.
- Krichevsky AM, Gabriely G. miR-21: a small multi-faceted RNA. *J Cell Mol Med* 2009;13:39–53.
- Chang Y, Jiang HJ, Sun XM, *et al*. Hepatic stellate cell-specific gene silencing induced by an artificial microRNA for antifibrosis *in vitro*. *Dig Dis Sci* 2010;55:642–653.
- Maubach G, Lim MC, Chen J, *et al*. miRNA studies in *in vitro* and *in vivo* activated hepatic stellate cells. *World J Gastroenterol* 2011;17:2748–2773.
- Marquez RT, Bandyopadhyay S, Wendlandt EB, *et al*. Correlation between microRNA expression levels and clinical parameters associated with chronic hepatitis C viral infection in humans. *Lab Invest* 2010;90:1727–1736.
- Kinnman N, Francoz C, Barbu V, *et al*. The myofibroblastic conversion of peribiliary fibrogenic cells distinct from hepatic stellate cells is stimulated by platelet-derived growth factor during liver fibrogenesis. *Lab Invest* 2003;83:163–173.
- Kinnman N, Gorla O, Wendum D, *et al*. Hepatic stellate cell proliferation is an early platelet-derived growth factor-mediated cellular event in rat cholestatic liver injury. *Lab Invest* 2001;81:1709–1716.
- Masyuk AI, Huang BQ, Ward CJ, *et al*. Biliary exosomes influence cholangiocyte regulatory mechanisms and proliferation through interaction with primary cilia. *Am J Physiol Gastrointest Liver Physiol* 2010;299:G990–G999.
- Castoldi M, Kordes C, Sawitza I, *et al*. Isolation and characterization of vesicular and non-vesicular microRNAs circulating in sera of partially hepatectomized rats. *Sci Rep* 2016;6:31869.